Supplementary Material

Performance of microAethalometers: Real-world Field Intercomparisons from Multiple Mobile Measurement Campaigns in Different Atmospheric Environments

Honey Dawn C. Alas[1*], Thomas Müller[1], Kay Weinhold[1], Sascha Pfeifer[1], Kristina Glojek[2], Asta Gregorič[3,4], Griša Močnik[3,5], Luka Drinovec[3,5], Francesca Costabile[6], Martina Ristorini[7], and Alfred Wiedensohler[1]

[1] *Leibniz Institute for Tropospheric Research, Leipzig, Germany*
[2] *Department of Geography, Faculty of Arts, University of Ljubljana, Ljubljana, Slovenia*
[3] *Center for Atmospheric Research, University of Nova Gorica, Ajdovščina, Slovenia*
[4] *Aerosol d.o.o., Kamniška 39 A, 1000 Ljubljana, Slovenia*
[5] *Condensed Matter Physics Department, J. Stefan Institute, Ljubljana, Slovenia*
[6] *Institute of Atmospheric Science and Climate, National Research Council, Rome, Italy*
[7] *Department of Bioscience and Territory, University of Molise, Pesche, Italy*

Table S1. Descriptive summary of the instruments used in this study.

Instrument	Platform	Operating principle	Light source wavelength	Time resolution
AE51	Mobile	Attenuation of light by particle loaded filter	880 nm	10 s
MA200	Mobile	Attenuation of light by particle loaded filter	375nm, 470 nm, 528 nm, 625 nm, 880 nm	10 s
MAAP	Fixed	Absorption of light by particle loaded filter. Multiangle absorption photometers allows for the use of the radiative transfer scheme to remove scattering effects	637 nm	60 s
AE33	Fixed	Attenuation of light by particle loaded filter	370, 470, 520, 590, 660, 880 and 950 nm	60 s

Table S2. Summary of the IC periods for each route.

IC locations	# of IC periods	Total IC period in minutes	# of filter changes
Manila campaign			
Katipunan Route			
(urban street)	32	222	77
(urban background)	73	128	
Taft Route	86	383	34
Rome campaign			
Rome city route	41	1116	77
Loški Potok campaign			
Village route			
(rural village)	102	2287	107
(rural background)	107	1166	

Table S3. Regression results for all AE51 correlations

Instrument	Study Area	IC Location	FLE Correction	Time of IC	Duration of IC	R^2	Slope	Time base	N (no. of IC points)
S5 vs S6	Rome		No			0.821	0.952 ± 0.003	10s	38909
	Loski Potok		No			0.972	1.003 ± 0.001	10s	27521
S5 vs Reference	Manila					0.367	0.879 ± 0.031	60s	1420
	Rome					0.985	1.017 ± 0.005	60s	772
	Loski Potok					0.985	0.808 ± 0.003	60s	1390
S6 vs Reference	Manila					NA	NA	60s	NA
	Rome					0.982	1.013 ± 0.004	60s	1157
	Loski Potok					0.973	0.841 ± 0.003	60s	3006
AE51 vs Reference	Loski Potok	Rural background				0.962	0.876 ± 0.005	60s	2888
		Rural village				0.978	0.826 ± 0.002	60s	1508
	Rome	Urban background				0.983	1.015 ± 0.003	60s	1929
	Manila	Urban background				0.845	0.871 ± 0.013	60s	815
		Urban street				0.545	1.55 ± 0.095	60s	222
		Urban street canyon				0.318	0.746 ± 0.056	60s	383
S5 vs Reference	Loski Potok	Rural background	No			0.965	0.876 ± 0.008	60s	475
			Yes			0.962	0.916 ± 0.008	60s	475
		Rural village	No			0.986	0.806 ± 0.003	60s	915
			Yes			0.99	0.951 ± 0.003	60s	915
S6 vs Reference		Rural background	No			0.96	0.876 ± 0.006	60s	1033
			Yes			0.959	0.934 ± 0.006	60s	1033
		Rural village	No			0.973	0.840 ± 0.003	60s	1973
			Yes			0.979	0.962 ± 0.003	60s	1973

Table S3 continued.

Instrument	Study Area	IC Location	FLE Correction	Time of IC	Duration of IC	R^2	Slope	Time base	N (no. of IC points)
AE51 vs Reference	Manila	Urban background	No	NN		0.726	0.905 ± 0.031	60s	325
		Urban street	No			0.409	1.518 ± 0.179	60s	105
		Urban street canyon	No			0.389	0.841 ± 0.078	60s	184
		Urban background	No	PM		0.888	0.862 ± 0.014	60s	490
		Urban street	No			0.709	1.573 ± 0.093	60s	117
		Urban street canyon	No			0.249	0.647 ± 0.081	60s	199
	Rome	Urban background	No	AM		0.988	1.022 ± 0.005	60s	718
			No	NN		0.939	0.941 ± 0.009	60s	747
			No	PM		0.975	1.006 ± 0.009	60s	464
	Loski Potok	Rural background	yes	AM		0.939	0.917 ± 0.010	60s	607
		Rural Village	yes			0.978	0.926 ± 0.004	60s	1202
		Rural background	yes	NN		0.978	0.894 ± 0.007	60s	353
		Rural Village	yes			0.972	0.917 ± 0.006	60s	692
		Rural background	yes	PM		0.954	0.975 ± 0.009	60s	549
		Rural Village	yes			0.989	0.976 ± 0.004	60s	994
S5 vs Reference			No		< 5 minutes	0.845	0.871 ± 0.013	60s	815
			yes		10 minutes	0.962	0.916 ± 0.008	60s	475
			yes		20 minutes	0.991	0.951 ± 0.003	60s	915
			No		30 minutes	0.985	1.017 ± 0.005	60s	772
S6 vs Reference			No		< 5 minutes	NA	NA	NA	NA
			yes		10 minutes	0.959	0.934 ± 0.006	60s	1033
			yes		20 minutes	0.979	0.962 ± 0.003	60s	1973
			No		30 minutes	0.982	1.013 ± 0.004	60s	1157

Table S4. Regression results for all MA200 correlations.

Instrument	IC Location	FLE Correction	Wavelength	R^2	Slope	Time base	N(no. of IC points)
MA200 75 vs 69			UV	0.876	1.083 ± 0.002	10s	27474
			Blue	0.574	1.121 ± 0.004	10s	
			Green	0.917	1.059 ± 0.002	10s	
			Red	0.929	1.051 ± 0.002	10s	
			IR	0.935	1.034 ± 0.002	10s	
MA200_75 vs AE51_S5			IR	0.917	0.965 ± 0.002	10s	30236
MA200_69 vs AE51_S6			IR	0.911	1.019 ± 0.001	10s	63495
MA200_69 vs Reference	Rural background	no	UV	0.887	0.681 ± 0.008	60s	930
			Blue	0.827	0.794 ± 0.012	60s	
			Green	0.931	0.830 ± 0.008	60s	
			Red	0.943	0.981 ± 0.008	60s	
			IR	0.952	1.026 ± 0.008	60s	
	Rural background	yes	UV	0.900	0.995 ± 0.001	60s	
			Blue	0.829	0.978 ± 0.015	60s	
			Green	0.938	0.976 ± 0.008	60s	
			Red	0.946	1.084 ± 0.009	60s	
			IR	0.952	1.097 ± 0.008	60s	
	Rural village	no	UV	0.798	0.369 ± 0.005	60s	1825
			Blue	0.670	0.480 ± 0.008	60s	
			Green	0.893	0.580 ± 0.005	60s	
			Red	0.922	0.747 ± 0.005	60s	
			IR	0.954	0.837 ± 0.005	60s	
	Rural village	yes	UV	0.935	0.854 ± 0.008	60s	
			Blue	0.810	0.842 ± 0.010	60s	
			Green	0.964	0.894 ± 0.005	60s	
			Red	0.967	0.999 ± 0.005	60s	
			IR	0.975	1.017 ± 0.004	60s	

Table S4 continued.

Instrument	IC Location	FLE Correction	Wavelength	R^2	Slope	Time base	N(no. of IC)
MA200_75 vs Reference	Rural background	no	UV	0.947	0.742 ± 0.008	60s	
			Blue	0.957	0.814 ± 0.008	60s	
			Green	0.961	0.881 ± 0.008	60s	
			Red	0.963	1.014 ± 0.010	60s	
			IR	0.965	1.013 ± 0.009	60s	445
	Rural background	yes	UV	0.941	1.087 ± 0.013	60s	
			Blue	0.957	1.022 ± 0.010	60s	
			Green	0.962	1.044 ± 0.010	60s	
			Red	0.964	1.117 ± 0.010	60s	
			IR	0.964	1.076 ± 0.010	60s	
	Rural village	no	UV	0.828	0.289 ± 0.005	60s	
			Blue	0.876	0.401 ± 0.005	60s	
			Green	0.899	0.471 ± 0.006	60s	
			Red	0.925	0.625 ± 0.006	60s	
			IR	0.957	0.743 ± 0.006	60s	
	Rural village	yes	UV	0.936	0.782 ± 0.007	60s	843
			Blue	0.956	0.821 ± 0.006	60s	
			Green	0.963	0.851 ± 0.006	60s	
			Red	0.968	0.924 ± 0.006	60s	
			IR	0.978	0.971 ± 0.006	60s	

Assessment of FLE in Manila and Rome datasets

Here, the details of the BC(ATN) approach performed to assess the FLE for the Manila and Rome datasets are presented. For the other two approaches, the information is provided in the Methods section of the main manuscript. They require the same data preparation as below.

For the BC(ATN), the 1-s raw data from the AE51 was compiled and given IDs pertaining to each mobile measurement period (1 completion of the route = 1 "run"). As ATN should start at 0 when the new filter is inserted at the start of each run, we deducted the initial value for each run (ATN at t=0, ATN0) from the ATN values during the measurements: the corrected ATN (ATNcorr) was calculated as the difference between the ATN measured at the next point in time (ATNt=1) and ATN0. ATN does not start at 0 when the filter is inserted due to ununiform illumination of the sample and reference spots in the filter photometers. Then, the BC mass concentrations were binned according to ATNcorr with intervals of 1 ATN. The BC mass concentration (with mean and median concentration per bin) was then plotted as a function of the ATNcorr. To detect the loading effect, a linear fit of both the mean and median values of the BC mass concentrations was performed over whole ATN range. Another experiment was to fit the mean and median values over only a specific ATN range. Drinovec et al. (2015) did not include the lowest and largest ATN values in the fitting due to low frequency of BC measurements at those values. In this study, we fitted the BC(ATN) plots only for BC values below the 95th percentile of the ATN. If the fit featured a negative slope, and BC is decreasing with increasing ATN, we interpreted this as the presence of the loading effect, that is the dependence of BC on ATN rather than just on the change of ATN in time. Normally, the loading parameter to correct the AE51 raw concentrations can be derived from the slope and intercept of the regression line.

Results of the FLE on AE51 data from Manila and Rome campaigns

In this section, the loading effect on the AE51 measurements from the Manila and Rome campaign was investigated following three approaches presented in the manuscript. The prerequisites for applying the filter loading effect correction using a loading parameter derived from a single period of analysis are having sufficient measurement data points and homogenous sources of particles.

For the BC(ATN) approach, again, the whole datasets (not just the data points during the intercomparison (IC) period) were used for a complete loading effect assessment. The results are shown in Figure S1. The blue and red dots represent the median and mean eBC mass concentration per ATN bin, respectively, while the error bars represent the standard deviation. To detect if there is a loading effect, a linear fit was performed over the whole ATN range and the ratio of the slope and the intercept represents the loading parameter k. If the slope of the fit is negative and its absolute value is greater than 0, then there is a loading effect.

However, Fig. S1 shows a positive slope which could be a statistical artifact (Drinovec et al., 2015).

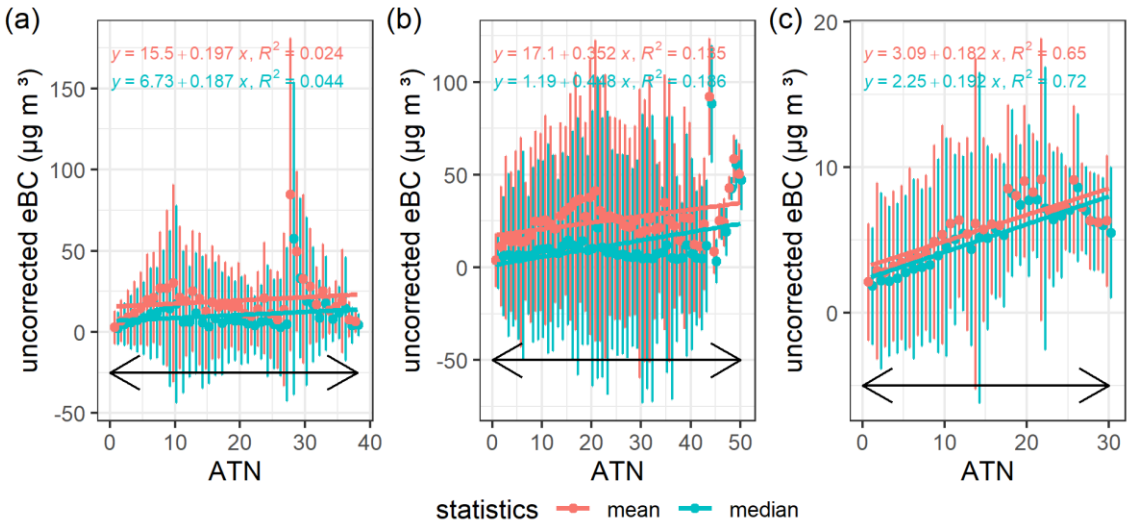

Figure S1 Binned raw measurements from the AE51 plotted against the attenuation (ATN) for a) Katipunan Route, b) Taft route, and c) Rome city route. Data were taken from the raw AE51 measurements (1-s resolution) from all the runs performed in each location (see Table S2), wherein a new filter was used for each run. The duration of a run is 1 hour for the Katipunan and Taft Route, and 2.5 hours for the Rome route. The blue and red dots represent the median and mean eBC mass concentration per bin, respectively, with the error bars as standard deviation. The solid lines are the linear fit for each statistic. The whole ATN range was used for linear fitting.

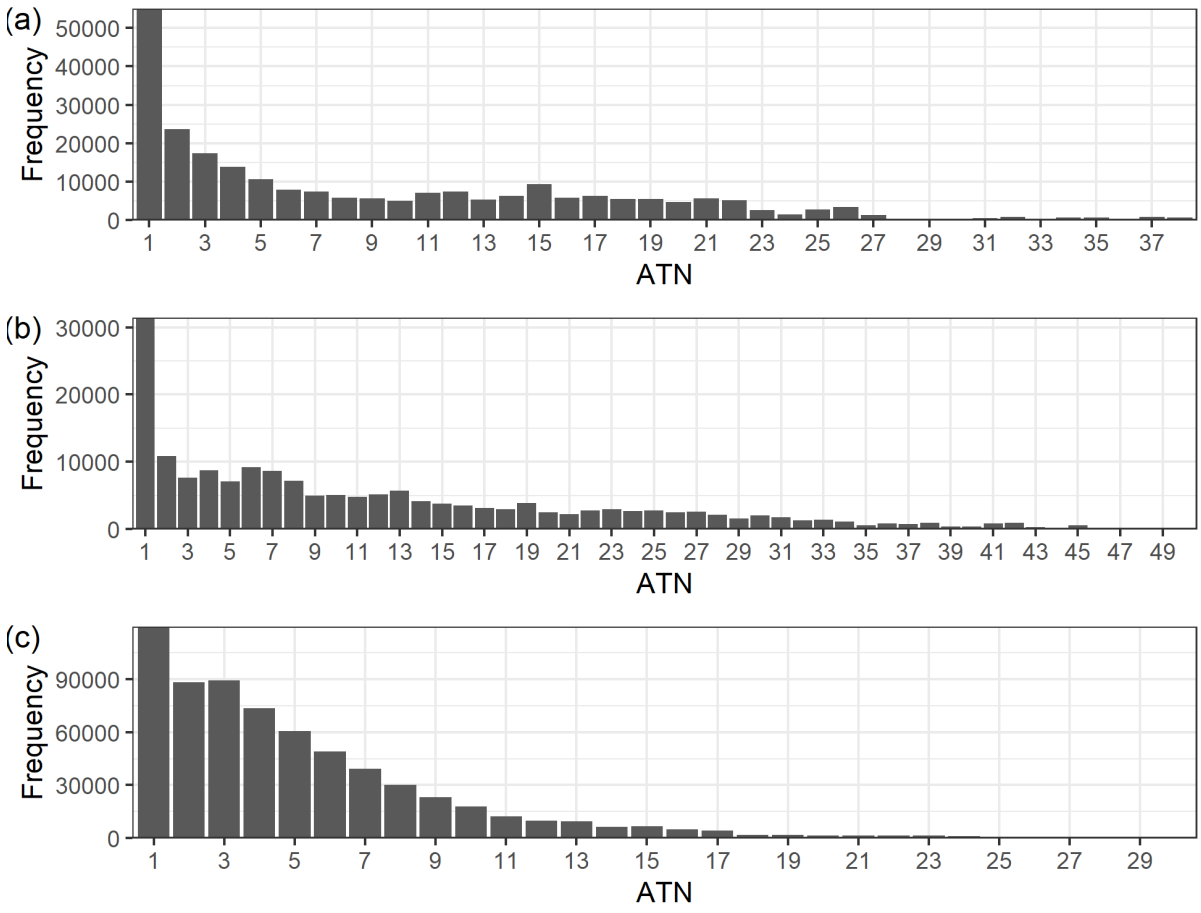

Figure S2 Frequency distributions of the measurements per ATN bin for the a) Katipunan Route, b) Taft route, and c) Rome city route.

Hence, to determine an appropriate range of ATN for fitting, the frequency distribution of the number of measurements per ATN bin was plotted and are shown in Figure S2. From here, the ATN range for fitting was adjusted to include only everything below the 95th percentile of the ATN as the frequency of the measurement decreases towards higher ATN.

The BC(ATN) was plotted again, this time fitting within the range of ATN reflecting 0-95th percentile of the data (Figure S3). For the Taft and Rome routes, the slopes are still positive. Refitting with ATN range down to < 85th percentile still resulted to positive slopes (not shown). For the Katipunan route, fitting the median values for an ATN range covering up to 95th and up to 85th percentile of the data gave negative slopes which could indicate a loading effect. However, from these plots, it can be observed that the dependency of BC on ATN seem to be affected by the route itself.

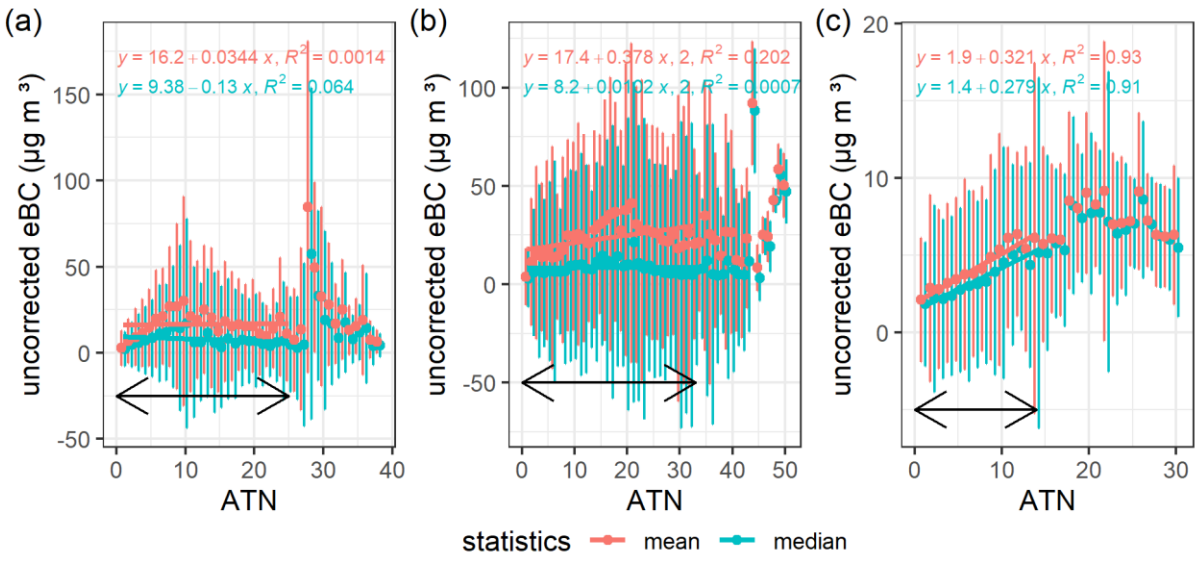

Figure S3 Same as Fig. S1 but this time the fit was only done on the data below the 95th percentile.

This indicates that there are clearly different sources throughout the route, which means probably different aerosol compositions. According to Drinovec et al., 2015, when the frequency distribution is not unimodal, this is indicative of different periods or in this case "area types" which could mean different source compositions and should be analyzed separately. However, as can be observed from Fig. S2, the number of measurements per ATN bin are not enough to derive loading parameters that are dependent on specific parts of the route.

The results of the deviation (ATN) approach are shown in Fig. S4. Figures on the left panel are AE51/Ref ratios vs AE51_ATN and on the right panels are AE51-Ref vs. AE51_ATN. The plots for the Katipunan dataset show inconclusive results with negative slope for the ratio vs ATN and positive for the difference vs ATN. The Taft dataset, on the other hand, show negative slopes for both, indicating a possible FLE. However, it must be noted that the number of datapoints used for this analysis is quite low (222 for Katipunan, and 383 for Taft) with the IC periods of less than 5 minutes each. This is evident in the figures with ratios much greater than 1 and large differences. As mentioned in the manuscript, the IC periods occurred in the middle

of a run, hence, this analysis do not cover a uniform dataset over the whole ATN range. Deriving a loading parameter from this analysis would also be misleading as we do not expect that the loading parameter in one point in space would be representative of the rest of the route in inhomogeneous atmospheres. The loading parameter depends on the whole collected sample on the spot.

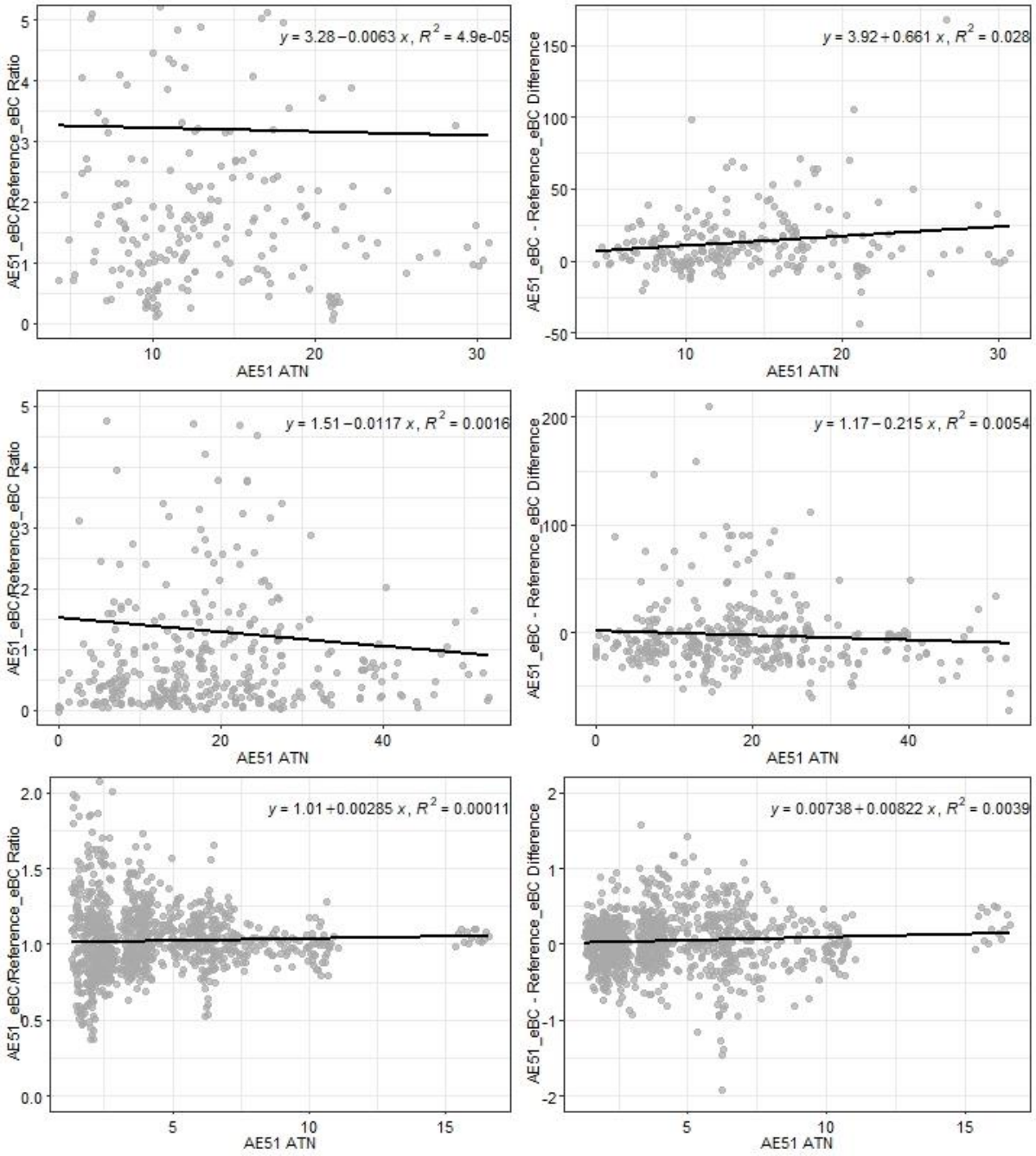

Figure S4 Scatter plots of the deviation between the AE51 and reference instruments expressed in ratios (left panels) and differences (right panels) for (a and b) the Katipunan (n = 222), (c and d) Taft (n = 383), and (e and f) Rome (n = 1116) datasets.

As a last attempt, a fixed k value of 0.005 was used to correct the Manila and Rome datasets (as was done for the Loški Potok AE51 data). This value represents the loading effect of a diesel exhaust dominated atmosphere as well as from fresh ambient wood burning (Drinovec et al., 2017). The corrected eBC was then plotted against the uncorrected eBC and is show in Fig. S5. This shows that the correction did not change the eBC measurements substantially (6%, 8%, and 3% overall differences between corrected and uncorrected measurements for the Katipunan, Taft, and Rome routes, respectively). As a result, no filter-loading effect correction was applied on the Manila and Rome datasets. As for the Manila dataset, the discrepancy between the mobile AE51 and the reference instrument is due to the high variabilities of different factors (wind, sources, etc.) characteristic of an urban area.

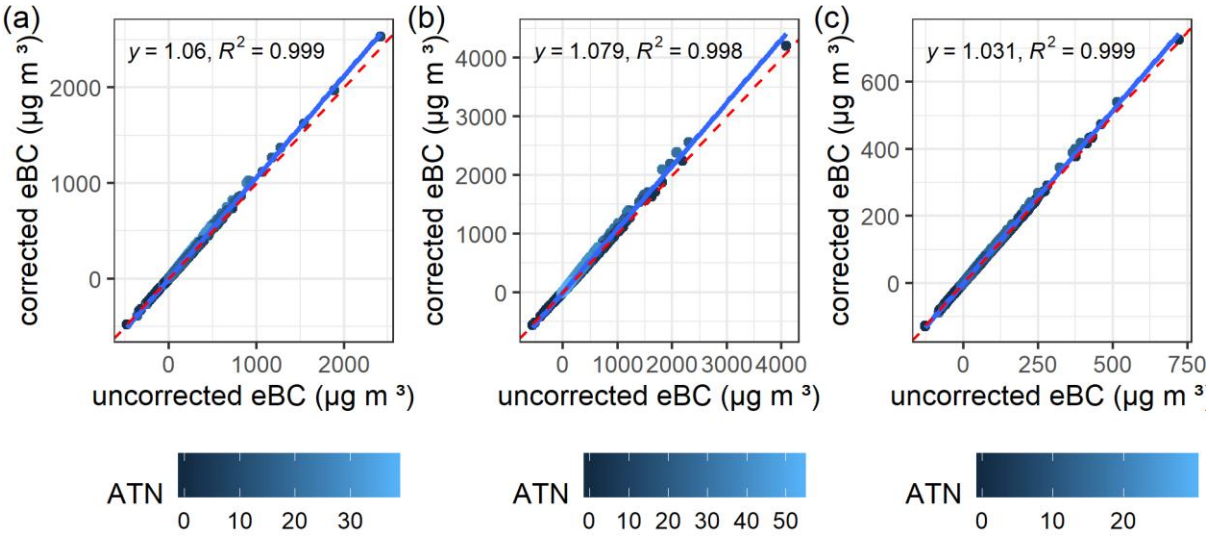

Figure S5 Correlation between the uncorrected and corrected (k = 0.005) eBC mass concentrations for the AE51 measurements along the a) Katipunan route, b) Taft route, and c) Rome route. The color of the dots represents the ATN. The red dashed line represents the 1:1 line, while the solid blue line represents the linear fit.

References

Drinovec, L., Gregorič, A., Zotter, P., Wolf, R., Bruns, E.A., Prévôt, A.S.H., Petit, J.-E., Favez, O., Sciare, J., Arnold, I.J., Chakrabarty, R.K., Moosmüller, H., Filep, A. and Močnik, G. (2017). The filter-loading effect by ambient aerosols in filter absorption photometers depends on the coating of the sampled particles. *Atmos. Meas. Tech.* 10: 1043-1059, https://doi.org/10.5194/amt-8-1965-2015.

Drinovec, L., Močnik, G., Zotter, P., Prévôt, A.S.H., Ruckstuhl, C., Coz, E., Rupakheti, M., Sciare, J., Müller, T., Wiedensohler, A. and Hansen, A.D.A. (2015). The "dual-spot" aethalometer: An improved measurement of aerosol black carbon with real-time loading compensation. *Atmos. Meas. Tech.* 8: 1965-1979, https://doi.org/10.5194/amt-10-1043-2017.